

# Entanglement Detection with Rotationally Covariant Measurements – From Compton Scattering to Lemonade

Marlene Funck,<sup>1</sup> Ilija Funk,<sup>2</sup> Tizian Schmidt,<sup>3</sup> and René Schwonnek<sup>1</sup>

<sup>1</sup>*Institut für Theoretische Physik, Leibniz Universität Hannover, Germany*

<sup>2</sup>*Institut für Quantenoptik, Leibniz Universität Hannover, Germany*

<sup>3</sup>*Institut für Festkörperphysik, Leibniz Universität Hannover, Germany*

(Dated: December 4, 2025)

The accurate and efficient detection of quantum entanglement remains a central challenge in quantum information science. In this work, we study the detection of entanglement of polarized photons for measurement devices that are solely specified by rotational symmetry. We derive explicit positive operator valued measures (POVMs) showing that from a quantum information perspective any such setting is classified by one real measurable parameter  $r$ . In Particular, we give a POVM formulation of the Klein–Nishina formula for Compton scattering of polarized photons. We provide an SDP-based entanglement certification method that operates on the full measured statistics and gives tight bounds, also considering semi-device independent scenarios. Furthermore, we show that, while Bell violations are impossible with rotationally covariant measurements, EPR steering can still be certified under one-sided symmetry constraints. Finally, we present a rotationally covariant showcase experiment, analyzing the scattering of polarized optical light in a selection of soft drinks. Our results suggest that lemonade-based detectors are suitable for entanglement detection.

## I. INTRODUCTION

Entanglement is the central phenomenon that separates quantum theory from a classical description of our world. Beyond this fundamental significance, it is also an essential resource for quantum technologies. This not only includes widely popular fields like quantum computing and cryptography, but also a less often highlighted medical application, positron emission tomography (PET) [1–13], which is one of the possible practical applications of the theory developed in this work.

Tackling the task of detecting and quantifying entanglement in a real-world experiment, one faces a fundamental challenge of theoretical physics: finding a model that is mathematically manageable and enables non-trivial conclusions, while not diverging (at least not significantly) from reality. For entanglement mediated by polarized photons, those models span a wide spectrum, ranging from minimal assumptions, like device-independent tests of Bell inequalities [14], to assuming idealized pure states and projective measurements [15]. While the first comes with very demanding technological requirements for any positive result [16–20], the latter will almost certainly fail to describe realistic experiments with unavoidable imperfections.

In this work, we develop and study a model at a useful middle ground: detecting entanglement of two polarized photons using measurement devices specified solely by rotational covariance, which can be found (or created) in a variety of settings (see Fig. 1). The primordial motivation of this work stems from Compton scattering experiments, used to detect correlations in  $\gamma$ -quanta. This mechanism was used in the very first quantum correlation experiments in the late 40’s [21], is today used to enhance PET scanners [1–12], and sparked a recent debate among theorists regarding the distinguishability of

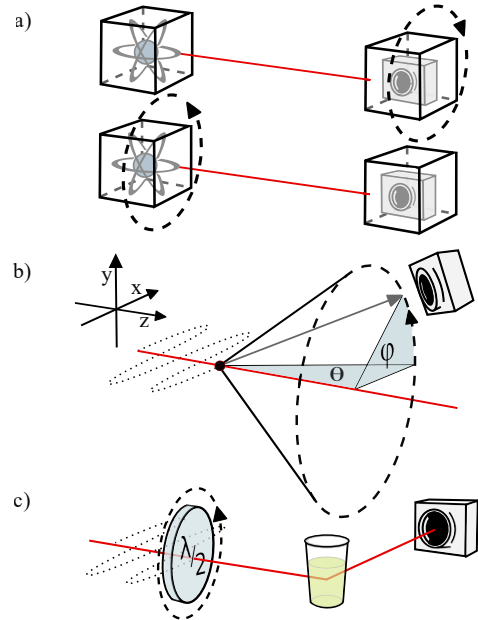


FIG. 1. a) Rotationally covariant measurement. Measurement data is  $2\pi$ -invariant. Rotating the preparation system (i.e. process before detection) or the detector are equivalent in description. b) Compton scattering process. Polarized photons scatter from electrons into angles,  $\theta$  and  $\varphi$ . It is rotationally covariant w.r.t.  $\varphi$ . c) The lemonade experiment. The polarization of photons is rotated by a half-wave plate. Photons scattered in the lemonade are detected at a fixed angle.

entangled and separable photon states in Compton scattering setups [1, 4, 22]. This is hopefully resolved now, as this paper shows that they can indeed be distinguished. Beyond this, rotational covariance can also be found in the mechanism that underpins the recent verification of entanglement at the LHC [23].

Since highly radioactive material or sufficiently large hadron colliders are rarely found in a standard laboratory for quantum optics, we introduce an easy-to-perform experiment analyzing scattering of photons with optical wavelengths (see Fig. 1c and Fig. 4). We measure the polarization dependent scattering distributions of a selection of soft drinks, and analyze them as rotational covariant detectors in our framework. Our results suggest that apple lemonade is suitable for detecting entanglement. In fact, the detection contrast obtained using lemonade-based detectors exceeds the known limit for Compton scattering of electron–positron annihilation photons. A fully conclusive experiment, however, demands entangled photon pairs and high sample sizes, which is why we leave it for a future publication.

Beyond serving as a neat showcase and potential student experiment, studying detectors based on soft drinks illustrates a conceptually central aspect of our work: It is unrealistic to find an exact model for a glass of lemonade, reflecting all relevant specifics and imperfections. Nevertheless, by reducing our description to a macroscopically implemented rotational symmetry, we are able to make a comprehensive analysis of the setup.

## II. BACKGROUND AND SETTING

Historically, the investigation of entanglement originates in the well-known Gedankenexperiment of Einstein, Podolski, Rosen [24] and Schrödinger [25], which predicted that quantum theory allows for correlations that cannot be explained classically. Already in 1950, Wu et al. [21] performed an experiment on Compton scattering of annihilation photons, which was recognized to be a proof of these correlations by Bohm and Aharonov [26] in 1957. Although their findings predated the more widely known Bell-type (CHSH: [14]) photon experiments by over a decade, they are rarely discussed in textbooks. One reason might be that the quantum information description of their setting is more subtle. In contrast to the CHSH setting, the Compton scattering measurement cannot be described by projective measurements typically used for discussing correlation tests. In fact, they are a prototype example of a joint measurement, where the traditional textbook postulate of a projection onto eigenstates fails. However, the language of quantum information has been developed further over the past decades [27–29] and provides the right tool for describing this setting: Quantum states are modeled by density operators  $\rho$ , which are positive unit trace operators acting on a Hilbert space  $\mathcal{H}$ . Measurement devices with outcomes in a measurable outcome set  $\Omega$  are modeled by positive operator-valued measures (POVMs), which assign a positive operator  $M[\omega]$  to every measurable subset  $\omega \subseteq \Omega$  with normalization  $M[\Omega] = 1$  such that  $\omega \mapsto \text{tr}[\rho M[\omega]]$  is a probability measure for every state  $\rho$  [30].

In the case of a bipartite setting, the Hilbert space factorizes:  $\mathcal{H} = \mathcal{H}_A \otimes \mathcal{H}_B$ . Local measurements  $M^{AB}$  are

modeled by a product of POVMs with outcomes  $\Omega_{AB} = \Omega_A \times \Omega_B$  and a decomposition  $M^{AB} = M^A \otimes M^B$ . A state  $\rho_{AB}$  is called separable, if it is a convex combination of product states [31], i.e.  $\rho_{AB} = \sum_i p_i \rho_A^i \otimes \rho_B^i$ , and entangled otherwise. The task of entanglement detection concerns the following prototypical question:

Given measurement data  $\Omega_{\text{meas}}$  observed on an unknown state  $\rho_{AB}$ . Can we find a separable state consistent with our observation – or – can we conclude that  $\rho_{AB}$  is entangled?

Recently, there has been renewed interest in analyzing entanglement in Compton scattering experiments, driven by its applications in medical imaging with positron emission tomography (PET) scanners [1–12, 32]. Hiesmayr et al. and Caradonna et al. [1–4] have proposed ways to describe the process from a quantum information perspective by reformulating the Klein–Nishina formula [33]. However, a precise description in quantum information language that rigorously distinguishes between the set of states (i.e., the preparation procedure) and the measurement devices (which are described by POVMs) was still lacking. This has caused confusion about the detectability of entanglement in previous works [1, 4, 22]. In this work, we derive and study the explicit POVMs for any setting with a rotational symmetry (in particular Compton scattering) and present an entanglement detection scheme that can be easily applied to them.

Our approach is based on two fundamental assumptions about the system and the measurement device:

- (i) The quantum state of the individual system can be described as a qubit.
- (ii) The system and measurement device are rotationally covariant (Fig. 1) with respect to  $U(1)$ .

In real-world experiments, assumption (i) is justified whenever the carrier of quantum information is a two-level system, transforming under the symmetry group  $SU(2)$ , or, in particular, the polarization of a single photon. When implementing this, e.g. with an SPDC source, this assumption translates as excluding the statistical influence of potential multi-photon events. This is reasonable as long as pump laser powers are kept sufficiently small so that the observed statistics are dominated by single-photon events. Assumption (ii) will be specified in chapter III.

In section III, we present the POVM description of a general rotationally covariant (RoC) measurement. Next, in section IV, we give a clear description of an entanglement detection procedure, including error handling. Section V elaborates on the semi-device independence of this approach, while section VI explains why this type of arrangement is unsuitable for Bell experiments, but it can demonstrate steering. In section VII, we use our formalism to recover well established descriptions of Compton scattering of polarized photons, like the Klein–Nishina Formula [33]. Finally, in section VIII, we introduce a simple experimental setup, described by our framework, using a laser, a half-wave plate, and a glass

of lemonade.

### III. ROTATIONALLY COVARIANT MEASUREMENTS

We make two basic assumptions: (i) that the preparation can be faithfully described as a qubit, and (ii) that the measurement is rotationally covariant (RoC). Considering experiments such as the Compton scattering (Fig. 1b), it is clear that the only action, an experimenter takes to switch between different observables, is to rotate some part of the measurement apparatus, for example, a detector (or a whole ring of them). Rotating by any angle  $\varphi$  will only cause the measurement data to shift cyclically, without actually changing the statistics.

Let  $\{U_\varphi\}_\varphi \subset \text{SU}(2)$  be the unitary action of the group of spacial rotations in  $\text{SO}(3)$  of an angle  $\varphi$  acting on the state space  $\mathbb{C}^2$ , i.e.

$$U_\varphi = e^{-i\varphi\sigma_z}, \quad \varphi \in [0, \pi), \quad (1)$$

where we fixed the rotational axis to be the z-axis.  $\sigma_z$  is the pauli matrix. Note that for a spin-1/2 system, one would get a factor of  $\frac{1}{2}$  in the exponent and have  $\varphi \in [0, 2\pi)$  instead.

We consider measurements, with outcome set  $\Omega = [0, \pi)$  and a POVM given by  $\text{M}[\omega] = \int_\omega M_\varphi d\varphi$  with an operator valued density  $M_\varphi$  yielding the probability density of a detection event at  $\varphi$ . We call a measurement with such a POVM *rotationally covariant*, if it fulfills

$$M_\varphi = \frac{1}{\pi} U_\varphi^* M_0 U_\varphi. \quad (2)$$

With this, the probability density of a detection event occurring at a differential angle segment  $d\varphi$  around  $\varphi$  for a given state  $\rho$  is

$$\mathbb{P}_\rho(d\varphi) = \frac{1}{\pi} \text{tr}[\rho U_\varphi^* M_0 U_\varphi] d\varphi. \quad (3)$$

The probability for an angle interval  $[\varphi_1, \varphi_2]$  is obtained by integrating (3) over that interval. By requiring that the total probability is normalized, we obtain the following form of  $M_0$  (details in VIII A):

$$M_0 = \mathbb{1} + r\sigma_x \quad r \in [0, 1], \quad (4)$$

where  $r$  is a setup-dependent parameter, which we call the ‘detector contrast’. A ‘perfect’ detector would be obtained for  $r = 1$ , while  $r = 0$  describes a detector measuring nothing but noise. Equations (2) and (4) show that any RoC measurement on a qubit is fully characterized by this one parameter  $r$ . This justifies the notation  $M_\varphi^r$  (and  $M_i^r$ ) for our POVM elements. As we will see, in the case of Compton polarimeters,  $r$  is the ‘analyzing power’.

Given an RoC device, the detector contrast  $r$  can be measured by using a source that emits a linearly polarized state (details in VIII B).

### IV. ENTANGLEMENT DETECTION FROM MEASURED DATA

Generally, entanglement detection is an NP-hard problem [34]. For two qubits, however, our formalism allows us to provide a straightforward method of determining whether the measured data corresponds to an entangled state. We do this by reformulating the task as a semidefinite program (SDP) [35] which is easily solved by, e.g., the MOSEK SDP solver with exact error estimations. Our reasons for choosing a numerical method are twofold. Firstly, the measurement record is structurally complex, and general binning over arbitrary angle segments prevents a compact analytical description. Secondly, we must incorporate optimization over finite sample errors, which SDPs handle naturally via convex confidence sets.

Assume that we have a bipartite system  $\rho \in \mathcal{H}_A \otimes \mathcal{H}_B$  with two parties, Alice and Bob, each holding a qubit and an RoC measurement device with a finite resolution. This is defined by a finite angle partition  $\{\Delta\varphi_i\}_{i \in I}$  ( $I$  being some index set) such that  $\cup_{i \in I} \Delta\varphi_i = [0, \pi)$ . Then Alice’s POVM is the set of operators

$$A_i = \int_{\Delta\varphi_i} \frac{1}{\pi} U_\varphi^* (\mathbb{1} + r_A \sigma_x) U_\varphi d\varphi, \quad i \in I \quad (5)$$

and Bob’s  $B_i$  respectively, where the detector contrasts  $(r_A, r_B)$  fully determine their measurement devices. Now the measurement statistic  $\{p_{ij}\}_{i,j \in I}$  for Alice detecting an event in  $\Delta\varphi_i$  and Bob simultaneously in  $\Delta\varphi_j$ , reflects the probabilities  $P_{ij} = \text{tr}[\rho (A_i \otimes B_j)]$  for a given state  $\rho$ .

We can make a statement about entanglement by solving a minimization problem: Let  $\mathcal{D}$  be the set of density matrices for a two-qubit system. Then the state is entangled, if

$$\inf\{\mathcal{N}(\tilde{\rho}) \mid \tilde{\rho} \in \mathcal{D}, \text{tr}[\tilde{\rho} (A_i \otimes B_j)] = p_{ij} \forall i, j\} > 0. \quad (6)$$

Here, we use the negativity  $\mathcal{N}(\rho) = \frac{\|\rho^\Gamma\|_1 - 1}{2} \geq 0$  [36], where  $\rho^\Gamma$  denotes the partial transpose of  $\rho$  on Alice’s part of the system and  $\|\cdot\|_1$  denotes the trace norm. It is a measure of entanglement with  $\mathcal{N}(\rho) > 0$ , if  $\rho$  is entangled. This minimization can be formulated as an SDP (derivation in VII C):

$$\inf\{\text{tr}[T] - 1 \mid \tilde{\rho}^\Gamma \leq T \geq 0, \text{tr}[\tilde{\rho} (A_i \otimes B_j)] = p_{ij} \forall i, j\}, \quad (7)$$

where the minimization runs over two matrices:  $T$  and the density matrices  $\tilde{\rho}$  compatible with the probabilities. We can detect entanglement by solving this SDP. Note, that for any  $r_A, r_B > 0$ , entanglement detection is equally possible. However, the statistical deviation of finite samples will scale with  $r_A, r_B$ .

When dealing with experimental data, we can take into account errors by assuming that the measurement data is independently and identically distributed (I.I.D.) and using Hoeffding’s inequality [37]. Choosing a confidence level  $c \in [0, 1]$ , we can estimate the probability  $\mathbb{P}$  that the deviation  $\varepsilon_{ij}$  of the experimental probabilities  $p_{ij}$  from the actual probabilities  $P_{ij}$  is smaller

than a  $c$ -dependent threshold (details in [VIIID](#)):

$$\mathbb{P}\left(\varepsilon_{ij} < \sqrt{\frac{n}{2} \ln \frac{2}{1-c}}\right) > c, \quad (8)$$

where  $n$  is the number of measurements. Both the negativity  $\mathcal{N}$  and the map  $\rho \rightarrow \text{tr}[\rho(A_i \otimes B_j)]$  are continuous with respect to the trace norm, so the maximum error in the negativity's minimum will be small for small  $\varepsilon_{ij}$ .

## V. SEMI-DEVICE INDEPENDENCE

It is possible to determine the detector contrast, if we are provided with perfectly prepared states. But what if we analyze top quarks or other systems that cannot be reliably prepared? Can we detect entanglement if the state and the RoC devices (i.e. the detector contrasts  $r_A, r_B$ ) are unknown? Indeed, we can. Our approach can detect entangled states without any knowledge of the devices involved. While it may not detect all entangled states, the detections it makes will be accurate.

The procedure is as follows: First, we have obtained the measurement statistics  $\{p_{ij}\}_{i,j}$ , where  $p_{ij} = \text{tr}[\rho(A_i^{r_A} \otimes B_i^{r_B})]$  for an unknown sample state  $\rho$  and unknown contrasts  $(r_A, r_B)$  of our sample devices. We now try to replicate these statistics using two arbitrary hypothetical RoC measurement devices, defined by  $(r_A^{\text{hyp}}, r_B^{\text{hyp}})$  and every hypothetical state  $\rho^{\text{hyp}}$ . Here, we can distinguish the following cases:

1.  $\{p_{ij}\}$  can only be replicated with entangled  $\rho^{\text{hyp}}$
2.  $\{p_{ij}\}$  can be replicated with some non-entangled  $\rho^{\text{hyp}}$
3.  $\{p_{ij}\}$  can not be replicated with any  $\rho^{\text{hyp}}$

When we say that the statistics are replicated, we mean that  $\text{tr}[\rho^{\text{hyp}}(A_i^{r_A^{\text{hyp}}} \otimes B_i^{r_B^{\text{hyp}}})] = p_{ij}$  holds for all  $i, j$ . For each hypothetical device  $(r_A^{\text{hyp}}, r_B^{\text{hyp}})$ , we can determine the case we are in by minimizing the SDP [\(7\)](#): If it returns minimal negativity  $\mathcal{N}_{\min} = 0$ , we are in case 2. If the minimum negativity is  $\mathcal{N}_{\min} > 0$ , we are in case 1. If it returns nothing, we are in case 3.

We know that the sample state  $\rho$  must have been entangled if, for all possible hypothetical devices  $(r_A^{\text{hyp}}, r_B^{\text{hyp}})$ , only case 1 and 3 appear. However, if case 2 appears – even for one hypothetical device – we cannot say with certainty that the state was entangled. Hence, this procedure allows for semi-device independence.

Assuming a maximally entangled sample state, we can derive the threshold below which device-independent entanglement detection is impossible. (details in [VIIIF](#)):

$$r_A r_B > \frac{1}{3}. \quad (9)$$

In particular, both sample detector contrasts  $r_A$  and  $r_B$  must be greater than  $1/3$ . Intuitively, the worse the contrast of the sample detectors, the more likely are false-negative results. Fig. 2 shows the correlation for the example of a maximally entangled sample state measured

with equal sample devices ( $r_A = r_B$ ). More details can be found in [VIIIE](#).

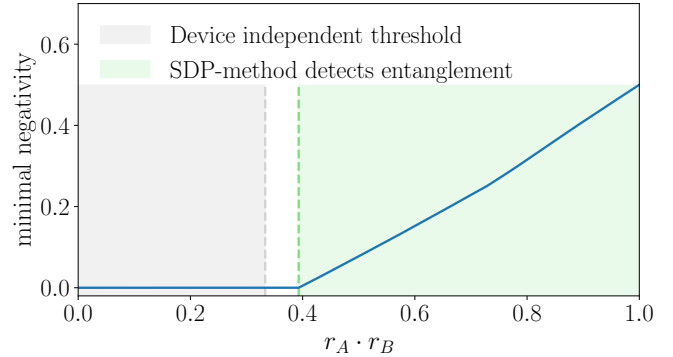


FIG. 2. Entanglement detection for equal sample devices  $r_A = r_B$  in the maximally entangled state  $|\Psi^-\rangle\langle\Psi^-|$ . The minimal negativities result from solving SDP [\(7\)](#) with perfect hypothetical devices  $r_A^{\text{hyp}} = r_B^{\text{hyp}} = 1$ , which, in this case, suffice as they yield the relevant results (see [VIIIE](#)). Entanglement detection is possible for those devices, where the minimal negativity is positive, in this scenario:  $r_A \cdot r_B \geq 0, 393$ .

## VI. BELL-EXPERIMENTS AND STEERING

We have established that our setting suffices to detect entanglement. A natural question arising is whether we can also observe steering or detect Bell violations, as these are the next items in the hierarchy.

With regard to steering, assume that Alice can perform  $\sigma_x$  and  $\sigma_y$  measurements, while Bob has some RoC device with detector contrast  $r$ . There are two cases to consider: Either  $r$  is known to Bob, or it is not. As shown in [VIIIG](#), if Bob knows the exact value of  $r$ , he can perform  $\sigma_x$  and  $\sigma_y$  measurements with the help of post-processing. Then the analogue of the CHSH-inequality for steering, which was shown by Cavalcanti et al. [\[38\]](#) becomes

$$\begin{aligned} & \sqrt{\langle(\sigma_x^A + \sigma_y^A)\sigma_x^B\rangle^2 + \langle(\sigma_x^A + \sigma_y^A)\sigma_y^B\rangle^2} \\ & + \sqrt{\langle(\sigma_x^A - \sigma_y^A)\sigma_x^B\rangle^2 + \langle(\sigma_x^A - \sigma_y^A)\sigma_y^B\rangle^2} \leq 2, \end{aligned} \quad (10)$$

where  $\langle\sigma_i^A\sigma_j^B\rangle = \text{tr}[\rho(\sigma_i^A \otimes \sigma_j^B)]$  for  $i, j \in \{x, y\}$ . For example, a Werner state  $\rho = f|\Psi^-\rangle\langle\Psi^-| + \frac{1-f}{4}\mathbb{1}$  yields  $\langle\sigma_i^A\sigma_j^B\rangle = -f\delta_{ij}$ , such that the left side of [\(10\)](#) becomes  $2\sqrt{2}f$ . This shows that, for known detector contrast  $r$ , we can demonstrate steering for Werner states with  $f > \frac{1}{\sqrt{2}}$ . If, on the other hand,  $r$  is unknown, then Bob's post-processed measurements are  $r\sigma_x^B$  and  $r\sigma_y^B$  (see [VIIIG](#)). In that case, for Werner states we obtain  $\langle\sigma_i^A r\sigma_j^B\rangle = -fr\delta_{ij}$  which yields  $2\sqrt{2}fr$  for the left side of [\(10\)](#). Therefore, steering can be demonstrated even if the exact value of  $r$  is unknown, provided that  $fr > \frac{1}{\sqrt{2}}$ .

To detect Bell violations, we can perform the standard CHSH experiment [\[14\]](#) (or any other Bell-type ex-

periment with an arbitrary number of measurement devices and outcomes) by selecting different angle partitions  $\{\Delta\varphi_i\}_{i \in I_A}$  defining Alice's (and Bob's) POVM as in (5).  $\{M_\varphi^{r_A}\}_{\varphi \in [0, \pi]}$  forms a parent POVM for all such measurements, which means that all POVM elements of Alice can be written as  $A_i = \int c_{\varphi, i|A} M_\varphi^r d\varphi$ , where  $c_{\varphi, i|A} \geq 0$  for each  $\varphi$  and measurement outcome  $i$  in measurement  $A$ , analogously for Bob. A simple calculation using the *Naimark Theorem* [39] for operator valued measures shows that this is enough to already know that a local hidden variable (LHV) model exists, and hence no Bell-violation is possible (details in **VIII H**).

## VII. RECOVERING THE KLEIN–NISHINA FORMULA FROM OUR FORMALISM

One example of a frequently discussed experiment that fits into our framework is the Compton scattering of linearly polarized photons on free electrons (Fig. 1b). Until today, the Klein–Nishina formula [33] is used to describe this setting [1, 4–7, 21, 22, 40, 41]. Although there are approaches for quantum information descriptions [1–4], an explicit formulation through POVMs is still missing. Our formalism can transfer specific descriptions like the Klein–Nishina formula to POVM-descriptions by simply adjusting the detector contrast  $r$ :

First, we consider the Klein–Nishina formula for linearly polarized photons scattered from an electron, which describes the intensity distribution  $I$  at azimuthal angle  $\theta$  and polar angle  $\varphi$  [33]:

$$I = \frac{f_0 \sin^2 \varphi}{(1 + \beta(1 - \cos \theta))^3} \left(1 + \frac{\beta^2(1 - \cos \theta)^2}{2 \sin^2 \varphi (1 + \beta(1 - \cos \theta))}\right). \quad (11)$$

Where  $f_0 = I_0 e^4 m_e^{-2} c^{-4} d^{-2}$  with  $I_0$  being the initial intensity,  $c$  the speed of light,  $m_e$  the electron mass, and  $d$  the distance between detector and scatterer.  $\beta = \hbar v m^{-1} c^{-2}$  is the quotient of the photon's and the electron's energy. As we show in **VIII I**, the probabilities of detecting a photon at angle  $\varphi$  (fixing  $\theta$ ) match the ones given by our RoC-framework, iff the detector contrast is

$$r(\beta, \theta) = \frac{1}{\beta(1 - \cos \theta) + 1 / (1 + \beta(1 - \cos \theta))}. \quad (12)$$

Thus, we can directly translate between the Klein–Nishina formula and our RoC-framework.

Secondly, we can recover the probabilities for case of positron–electron annihilation photons (which are orthogonally linearly polarized) being Compton scattered into two directions described by the azimuthal angles  $\theta_A$ ,  $\theta_B$  and  $\Delta\varphi = \varphi_B - \varphi_A$ , the angle between their scattering planes (see Fig. 3). There has been a vast amount of experiments and theoretical work, e.g., about correlations in this process [1, 4, 5, 22, 40, 42–45]. It is usually described by a probability distribution, sometimes called Pryce–Ward–equation after [42]. When fixing both the

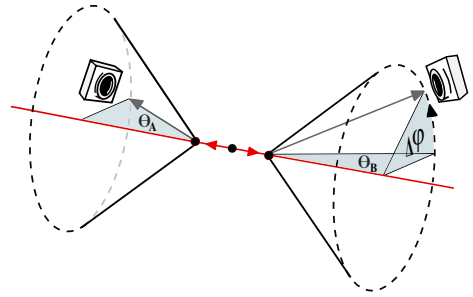


FIG. 3. Two Compton polarimeters. A source emits orthogonally linearly polarized (entangled) photons which scatter from electrons. Coincidence events of the photons that are scattered in directions  $(\theta_A, 0)$  and  $(\theta_B, \Delta\varphi)$  are detected.

photon energy and the azimuthal angles  $\theta_i$ , renormalization yields

$$\mathbb{P}_{\theta_A, \theta_B}(\Delta\varphi) = \frac{1}{\pi} [1 - \alpha(\theta_A)\alpha(\theta_B) \cos(2\Delta\varphi)]. \quad (13)$$

$\alpha(\theta_A)$  and  $\alpha(\theta_B)$  are the analyzing powers of the Compton polarimeters [6]. Defining the orthogonally linearly polarized photon state as the pure state  $\rho_\perp$  given by  $\frac{1}{\sqrt{2}}(|HV\rangle - |VH\rangle)$ , the RoC framework yields the probability

$$\begin{aligned} \mathbb{P}_{r_A r_B}^{\text{RoC}}(\Delta\varphi) &= \int_0^\pi \frac{\text{tr}[\rho_\perp (M_\varphi^{r_A} \otimes M_{\varphi+\Delta\varphi}^{r_B})]}{\pi^2} d\varphi \\ &= \frac{2}{\pi} [1 - r_A r_B \cos(2\Delta\varphi)]. \end{aligned} \quad (14)$$

Hence, we can reproduce (13) for  $r_i = \alpha(\theta_i)$ . According to [22, 46] the maximal value of  $\alpha(\theta_i)$  (and hence  $r_i$ ) in this particular setting is 0.69. For known  $r$ , we can use the entanglement detection scheme in **IV**. Our analysis from **V** shows that this setting can even do semi-device independent entanglement detection: For the best-case scenario,  $r_A = r_B = 0.69$ , entanglement in e.g. Werner states can be detected for  $f > 0.8$  (analogously to Fig. 2).

Derivation (14) settles the dispute between [1, 4, 22] regarding the distinguishability of separable and entangled orthogonally polarized states, namely,  $\rho_\perp$  from above and the separable state  $\rho_{\text{mix}} = (|VH\rangle\langle VH| + |HV\rangle\langle HV|)/2$ . For  $\rho_{\text{mix}}$ , the same derivation as in (14) yields an angle-independent distribution ( $\mathbb{P}_{r_A r_B}^{\text{RoC}}(\Delta\varphi) = \frac{1}{\pi}$ ). This is in agreement with Caradonna et al. [1] and the results of Bohm and Aharonov [26].

Thirdly, when analyzing the above scattering towards correlations, in many cases the fraction  $R$  of perpendicular and parallel scattering events is considered [2, 6, 22, 40, 42, 47–50]. Again, this can be derived easily with our framework, using (14):

$$R = \frac{\mathbb{P}_{r_A r_B}^{\text{RoC}}(\pi/2)}{\mathbb{P}_{r_A r_B}^{\text{RoC}}(0)} = \frac{1 + r_A r_B}{1 - r_A r_B}. \quad (15)$$

In summary, our formalism is well suited for ongoing discussions, especially about quantum correlations. The

methods presented in III, IV and V, allow for a simple yet precise analysis of quantum correlations, offering a more comprehensive perspective than case-specific descriptions, which often fail to capture the whole picture.

### VIII. SOFT-DRINK-BASED DETECTORS

We now introduce a simple showcase experiment based on photon-scattering from a selection of soft drinks that demonstrates how our formalism can be easily applied. First, note that the polarization of a photon can be described as a qubit, and that linear polarization can be rotated with a half-wave plate (see Fig. 1c). When being shot at suitable liquids, linearly polarized photons scatter polarization-dependently, which yields a power distribution over the angles  $\varphi \in [0, 2\pi)$ . In accordance with our symmetry assumptions, instead of measuring this distribution with a detector rotating around the scatterer, one can rotate the wave plate (and thus the incident polarization), while keeping the detector at a fixed angle. The performed experiment is visualized in Fig. 4. Note that the photons are emitted by a 30 mW continuous-wave laser with a beam diameter of 5 mm. Although the laser is not a single-photon source, we operate far below any optical nonlinearity, such that the scattering behavior and hence the determined parameter  $r$  can be directly extrapolated to single-photon measurements.

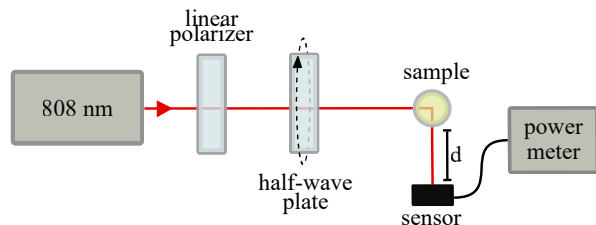


FIG. 4. The experiment: A single mode, fiber-coupled, 30 mW power, 808 nm, continuous-wave diode laser, followed by a linear polarizer (anti-reflection coated for 808 nm) with an extinction ratio of  $10^8:1$ . The polarization is rotated by a half-wave plate (anti-reflection coated for 808 nm). The light scatters from different sample liquids contained in a glass test tube (diameter: 25 mm) and is measured roughly at a right angle compared to the incoming beam using an optical power meter. Powers were measured with an integration time of 1 s.

The complex composition of the molecules, particles and bubbles found in some of the examined liquids, makes it difficult to determine the relative contributions of Rayleigh, Mie and geometric scattering. However, by construction, our approach remains valid even without a detailed model of the underlying scattering mechanisms or the specific geometry of the setup, as it only depends on the realization of the rotational symmetry: The distribution we expect for the linearly polarized state

Liquid	Detector contrast $r$ from fit
Elderflower sirup	$0.246 \pm 0.001$
Fanta-lemon	$0.390 \pm 0.001$
Vitamin water	$0.395 \pm 0.001$
Maracuja lemonade	$0.489 \pm 0.001$
Grapefruit lemonade	$0.498 \pm 0.001$
Apple lemonade	$0.610 \pm 0.001$

TABLE I. Changing the liquid sample significantly influences the measured detector contrast  $r$ . The measurements were performed with a fixed detector distance  $d = 20$  mm.  $r$  was obtained by fitting the data to  $f(\varphi) = a(1+r \cos(2(\varphi + \varphi_0)))$ . The dominant contribution to the uncertainty of  $r$  arises from the laser intensity stability.

$\rho_{\text{lin}} = \frac{1}{2}\mathbb{1} + \frac{1}{2}\sigma_x$  is described by the RoC-POVM (2):

$$P_{\rho_{\text{lin}}}^r(\varphi) = \text{tr}[\rho_{\text{lin}} M_\varphi^r] = \frac{1 + r \cos(2\varphi)}{2\pi}. \quad (16)$$

By fitting the measurement data to (16), we can determine the detector contrast  $r$  of this setup. It is influenced by, e.g., the detector distance  $d$ , the diameter of the test tube, laser stability, detector efficiency, but also, to a large extent, by the selected sample liquid. The results in (Table I) show that, in a fixed setup, we can change the detector contrast within a wide range by changing the sample liquid. These measurements were done for  $d = 20$  mm, with the dominant contribution to the uncertainty of  $r$  arising from the laser intensity stability. As a second step, the detector contrast  $r$  was further increased by reducing the distance between the detector and the liquid from  $d = 20$  mm to  $d = 15$  mm. The corresponding results, showing the measured scattered output power as a function of the angle, are presented in Fig. 5.

Using apple lemonade as a scatterer, we find that a detector contrast of at least  $r = 0.704 \pm 0.001$  can be achieved, which is higher than the known theoretical upper bound for Compton scattering experiments of positron-electron annihilation photons (VII). While any characterized detector with  $r > 0$  can detect entanglement, see IV, a lemonade-based detector with this quality even suffices to detect entanglement in the semi-device independent setting described in V. Recall that the threshold for semi-device independent entanglement detection with equal devices is  $r_{\text{thresh}} = \sqrt{0.393} \approx 0.627$  (see Fig. 2), assuming a maximally entangled state. In contrast, two identical detectors with  $r = 0.704$  can even detect entanglement of Werner states, with fidelity  $f \geq 0.795$  (this corresponds to an achievable score of  $S \geq 2.249$  in a CHSH inequality).

One way to implement an entanglement detection scheme is to use entangled photon pairs generated by spontaneous parametric down-conversion and hand Alice and Bob each a glass of lemonade. This is feasible in practice, as entanglement sources with the required fidelity are widely available. The measured distribution of coincidence events in all angle segments can then be

used to solve the SDP (7). Of course, achieving a sufficiently high rate of coincidence events such that the experiment is feasible in a reasonable time frame is challenging. Nonetheless, our findings indeed give no reason to believe that entanglement detection with lemonade should be ruled out.

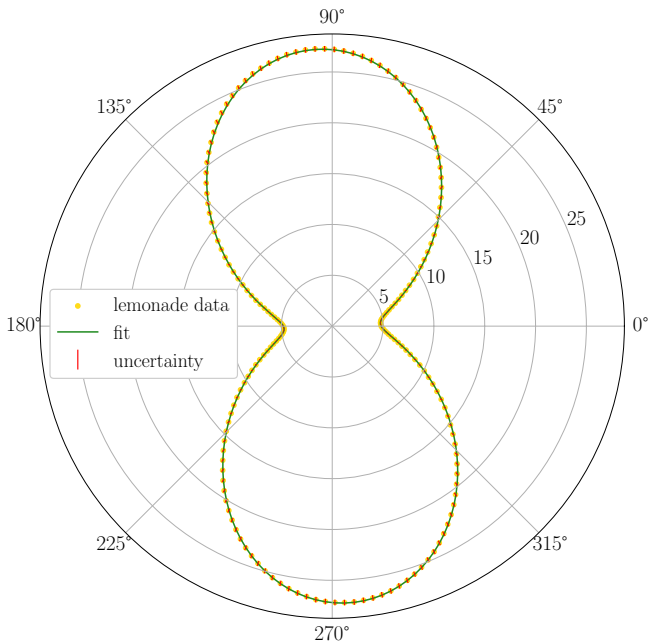


FIG. 5. Scattered power distribution in mW for apple lemonade, resulting in  $r = 0.704 \pm 0.001$ , measured at a distance of  $d = 15$  mm.  $r$  was obtained by fitting the data to  $f(\varphi) = a(1 + r \cos(2(\varphi + \varphi_0)))$ . The dominant contribution to the uncertainty of  $r$  arises from the laser intensity stability.

## CONCLUSION

Our work opens the door to a clean, quantum information analysis of rotationally covariant single photon

experiments. In particular, we derived the POVM-formulation of the Klein–Nishina formula, describing Compton scattering of polarized photons. In fact, we found that RoC measurements are indistinguishable from a quantum information perspective, as they are fully classified by the established detector contrast  $r$ , determining the quality of the measurement. Furthermore, we have introduced an entanglement certification method for RoC measurements, only requiring the measured data and an SDP solver, and have generalized this method for unknown detector contrasts  $r$ . We have shown that any RoC setup admits a parent POVM and is hence not suitable for Bell–violations, while steering with one characterized RoC measurement is possible.

One direction for future work is the analysis of U(1) representations beyond qubits, by analyzing U(1) symmetries on multi-photon states and on arbitrary systems. Another direction is to extend this analysis to detectors that omit an O(3) covariance. Those are, for example, natural for scattering experiments, in which the detector is rotated on two angles (see Fig. 1b). Additionally, one could test the predictions of the Klein–Nishina Formula with our framework. Lastly, our hope is to enable entanglement detection with our introduced lemonade-experiment.

## ACKNOWLEDGMENTS

We gratefully acknowledge discussions with Otfried Gühne, Mathias Kleinmann, Robert Raußendorf, and Tobias Osborne. MF acknowledges helpful comments by Lukas Hantzko, Lennart Binkowski, and Hauke Hinrichs. MF and RS acknowledge support by the Quantum Valley Lower Saxony, the Cluster of Excellence Quantum Frontiers, and by the BMBF projects ATIQ, QUIX, SEQUIN and CBQD.

---

[1] P. Caradonna, D. Reutens, T. Takahashi, S. Takeda, and V. Vegh, Probing entanglement in compton interactions, *Journal of Physics Communications* **3**, 105005 (2019).

[2] P. Caradonna, I. D’amico, D. Jenkins, and D. Watts, Stokes-parameter representation for compton scattering of entangled and classically correlated two-photon systems, *Physical Review A* **109**, 033719 (2024).

[3] P. Caradonna, Compton scattering mediated by quantum entanglement, *Physical Review A* **111**, 053708 (2025).

[4] B. Hiesmayr and P. Moskal, Witnessing entanglement in compton scattering processes via mutually unbiased bases, *Scientific Reports* **9** (2019).

[5] D. Watts, J. Bordes, J. Brown, A. Cherlin, R. Newton, J. Allison, M. Bashkanov, N. Efthimiou, and N. Zachariou, Photon quantum entanglement in the mev regime and its application in pet imaging, *Nature communications* **12**, 2646 (2021).

[6] D. Abdurashitov, A. Baranov, D. Borisenco, F. Guber, A. Ivashkin, S. Morozov, S. Musin, A. Strizhak, I. Tkachev, V. Volkov, and B. Zhuikov, Setup of compton polarimeters for measuring entangled annihilation photons, *Journal of Instrumentation* **17** (03), P03010.

[7] H. Zaidi and K. F. Koral, Scatter modelling and compensation in emission tomography, *European journal of nuclear medicine and molecular imaging* **31**, 761 (2004).

[8] G. Romanchek, G. Shoop, and S. Abbaszadeh, Application of quantum entanglement induced polarization for dual-positron and prompt gamma imaging, *Bio-algorithms and med-systems* **19**, 9 (2023).

[9] G. Romanchek, G. Shoop, K. Gholami, E. Enlow, and

S. Abbaszadeh, Quantum entanglement filtering: A pet feasibility study in imaging dual-positron and prompt gamma emission via monte carlo simulation, IEEE transactions on radiation and plasma medical sciences (2024).

[10] D. Kim, A. N. Rachman, U. Taisei, M. Uenomachi, K. Shimazoe, and H. Takahashi, Background reduction in pet by double compton scattering of quantum entangled annihilation photons, *Journal of Instrumentation* **18** (07), P07007.

[11] H. Eslami and M. Mohamadian, Optimization of the positron emission tomography image resolution by using quantum entanglement concept, *The European Physical Journal Plus* **139**, 976 (2024).

[12] P. Moskal, D. Kumar, S. Sharma, E. Y. Beyene, N. Chug, A. Coussat, C. Curceanu, E. Czerwiński, M. Das, K. Dulski, *et al.*, Nonmaximal entanglement of photons from positron-electron annihilation demonstrated using a plastic pet scanner, *Science Advances* **11**, eads3046 (2025).

[13] A. McNamara, M. Toghiani, J. Gillam, K. Wu, and Z. Kuncic, Towards optimal imaging with pet: an in silico feasibility study, *Physics in Medicine & Biology* **59**, 7587 (2014).

[14] J. F. Clauser, M. A. Horne, A. Shimony, and R. A. Holt, Proposed experiment to test local hidden-variable theories, *Physical review letters* **23**, 880 (1969).

[15] C. Cohen-Tannoudji, B. Diu, and F. Laloë, *Quantum mechanics, volume 3: fermions, bosons, photons, correlations, and entanglement* (John Wiley & Sons, 2019).

[16] M. Giustina, A. Mech, S. Ramelow, B. Wittmann, J. Kofler, J. Beyer, A. E. Lita, B. Calkins, T. Gerrits, S. W. Nam, R. Ursin, T. Scheidl, J. Handsteiner, F. Steinlechner, C. Abellán, W. Amaya, V. Pruneri, M. W. Mitchell, and A. Zeilinger, Bell violation using entangled photons without the fair-sampling assumption, *Nature* **497**, 227 (2013).

[17] O. Gühne, Detecting quantum entanglement: entanglement witnesses and uncertainty relations, (2004).

[18] M. Giustina, M. A. M. Versteegh, S. Wengerowsky, J. Handsteiner, A. Hochrainer, K. Phelan, F. Steinlechner, J. Kofler, J.-. Larsson, C. Abellán, W. Amaya, V. Pruneri, M. W. Mitchell, J. Beyer, T. Gerrits, A. E. Lita, L. K. Shalm, S. W. Nam, T. Scheidl, R. Ursin, B. Wittmann, and A. Zeilinger, Significant-loophole-free test of bell's theorem with entangled photons, *Phys. Rev. Lett.* **115**, 250401 (2015).

[19] L. Shalm, E. Meyer-Scott, B. Christensen, P. Bierhorst, M. Wayne, M. Stevens, T. Gerrits, S. Glancy, D. Hamel, M. Allman, K. Coakley, S. Dyer, C. Hodge, A. Lita, V. Verma, C. Lambrocco, E. Tortorici, A. Migdall, Y. Zhang, D. Kumor, W. Farr, F. Marsili, M. Shaw, J. Stern, C. Abellán, W. Amaya, V. Pruneri, T. Jennewein, M. Mitchell, P. Kwiat, J. Bienfang, R. Mirin, E. Knill, and S. Nam, Strong loophole-free test of local realism, *Phys. Rev. Lett.* **115**, 250402 (2015).

[20] B. Hensen, H. Bernien, A. . Dréau, A. Reiserer, N. Kalb, M. S. Blok, J. Ruitenberg, R. F. L. Vermeulen, R. N. Schouten, C. Abellán, W. Amaya, V. Pruneri, M. W. Mitchell, M. Markham, D. J. Twitchen, D. Elkouss, S. Wehner, T. H. Taminiau, and R. Hanson, Loophole-free bell inequality violation using electron spins separated by 1.3 km, *Nature* **526**, 682 (2015).

[21] C. S. Wu and I. Shaknov, The angular correlation of scattered annihilation radiation, *Phys. Rev.* **77**, 136 (1950).

[22] A. Ivashkin, D. Abdurashitov, A. Baranov, F. Guber, S. Morozov, S. Musin, A. Strizhak, and I. Tkachev, Testing entanglement of annihilation photons, *Scientific reports* **13**, 7559 (2023).

[23] Y. Afik and J. R. M. de Nova, Entanglement and quantum tomography with top quarks at the lhc, *The European Physical Journal Plus* **136**, 907 (2021).

[24] A. Einstein, B. Podolsky, and N. Rosen, Can quantum-mechanical description of physical reality be considered complete?, *Phys. Rev.* **47**, 777 (1935).

[25] E. Schrödinger, Die gegenwärtige situation in der quantenmechanik, *Naturwissenschaften* **23**, 844 (1935).

[26] D. Bohm and Y. Aharonov, Discussion of experimental proof for the paradox of einstein, rosen, and podolsky, *Phys. Rev.* **108**, 1070 (1957).

[27] R. F. Werner, Quantum states with einstein-podolsky-rosen correlations admitting a hidden-variable model, *Physical Review A* **40**, 4277 (1989).

[28] G. Ludwig, *Foundations of quantum mechanics I* (Springer Science & Business Media, 2012).

[29] K. Kraus, A. Böhm, J. D. Dollard, and W. Wootters, *States, effects, and operations fundamental notions of quantum theory: Lectures in mathematical physics at the university of Texas at Austin* (Springer, 1983).

[30] T. Heinosaari and M. Ziman, *The mathematical language of quantum theory: from uncertainty to entanglement* (Cambridge University Press, 2011).

[31] R. F. Werner, Quantum states with einstein-podolsky-rosen correlations admitting a hidden-variable model, *Phys. Rev. A* **40**, 4277 (1989).

[32] G. R. Romanek, G. Shoop, M. A. Kupinski, P. H. Kuo, M. King, L. R. Furenlid, and S. Abbaszadeh, Investigation of quantum entanglement information for  $\beta$ - $\gamma$  coincidences, *Bio-Algorithms and Med-Systems* **20**, 27 (2024).

[33] O. Klein and Y. Nishina, Über die streuung von strahlung durch freie elektronen nach der neuen relativistischen quantendynamik von dirac, *Zeitschrift für Physik* **52**, 853 (1929).

[34] L. Gurvits, Classical complexity and quantum entanglement, *Journal of Computer and System Sciences* **69**, 448 (2004), special Issue on STOC 2003.

[35] S. P. Boyd and L. Vandenberghe, *Convex optimization* (Cambridge university press, 2004).

[36] G. Vidal and R. F. Werner, Computable measure of entanglement, *Physical Review A* **65**, 032314 (2002).

[37] W. Hoeffding, Probability inequalities for sums of bounded random variables, *The collected works of Wassily Hoeffding* , 409 (1994).

[38] E. G. Cavalcanti, C. J. Foster, M. Fuwa, and H. M. Wiseman, Analog of the clauser–horne–shimony–holt inequality for steering, *Journal of the Optical Society of America B* **32**, A74 (2015).

[39] A. Peres, *Quantum theory: concepts and methods* (Springer, 2002).

[40] L. Kasday, J. Ullman, and C. Wu, Angular correlation of compton-scattered annihilation photons and hidden variables, *Il Nuovo Cimento B (1971-1996)* **25**, 633 (1975).

[41] A. Strizhak, D. Abdurashitov, A. Baranov, A. Ivashkin, and S. Musin, Study of the compton scattering of entangled annihilation photons, *Physics of Particles and Nuclei Letters* **19**, 509 (2022).

[42] M. Pryce and J. Ward, Angular correlation effects with annihilation radiation, *Nature* **160**, 435 (1947).

[43] S. Parashari, D. Bosnar, I. Friščić, A. M. Kožuljević,

Z. Kuncic, P. Žugec, and M. Makek, Closing the door on the “puzzle of decoherence” of annihilation quanta, *Physics Letters B* **852**, 138628 (2024).

[44] I. Tkachev, S. Musin, D. Abdurashitov, A. Baranov, F. Guber, A. Ivashkin, and A. Strizhak, Measuring the evolution of entanglement in compton scattering, *Scientific Reports* **15**, 6064 (2025).

[45] P. Moskal, D. Kumar, S. Sharma, E. Y. Beyene, N. Chug, A. Coussat, C. Curceanu, E. Czerwiński, M. Das, K. Dulski, *et al.*, Nonmaximal entanglement of photons from positron-electron annihilation demonstrated using a plastic pet scanner, *Science Advances* **11**, eads3046 (2025).

[46] H. S. Snyder, S. Pasternack, and J. Hornbostel, Angular correlation of scattered annihilation radiation, *Phys. Rev.* **73**, 440 (1948).

[47] M. Bruno, M. d’Agostino, and C. Maroni, Measurement of linear polarization of positron annihilation photons, II *Nuovo Cimento B Series 11* **40**, 143 (1977).

[48] A. Wilson, J. Lowe, and D. Butt, Measurement of the relative planes of polarization of annihilation quanta as a function of separation distance, *Journal of Physics G: Nuclear Physics* **2**, 613 (1976).

[49] H. Langhoff, Die linearpolarisation der vernichtungsstrahlung von positronen, *Zeitschrift für Physik* **160**, 186 (1960).

[50] G. Faraci, D. Gutkowski, S. Notarrigo, and A. Peninisi, An experimental test of the epr paradox, *Lettore al Nuovo Cimento (1971-1985)* **9**, 607 (1974).

[51] A. S. Holevo, *Probabilistic and statistical aspects of quantum theory*, Vol. 1 (Springer Science & Business Media, 2011).

## METHODS

### A. Derivation of $M_0$

We derive (4): Dealing with a probability distribution, we assume

$$\begin{aligned} 1 = \mathbb{P}_\rho([0, \pi]) &= \int_0^\pi \frac{1}{\pi} \text{tr}[\rho U_\varphi^* M_0 U_\varphi] d\varphi \\ &= \text{tr}[M_0 \int_0^\pi \frac{1}{\pi} U_\varphi \rho U_\varphi^* d\varphi] \\ &= \text{tr}[M_0 \bar{\rho}], \end{aligned} \quad (17)$$

where  $\bar{\rho} = \frac{1}{2}(\mathbb{1} + \alpha \sigma_z)$  is the density matrix averaged over all possible rotations along the z-axis ( $\alpha \in [-1, 1]$ ). This must hold for any state  $\rho$ , so

$$1 = \frac{1}{2} \text{tr}[M_0(\mathbb{1} + \alpha \sigma_z)] \quad \forall \alpha \in [-1, 1] \quad (18)$$

Since  $M_0$  is positive (and hermitian), it can be written in the form  $M_0 = \lambda \mathbb{1} + \vec{k} \vec{\sigma}$  for some real  $\lambda$  and  $\vec{k}$  with  $|\vec{k}|^2 = k_x^2 + k_y^2 + k_z^2 \leq \lambda^2$ . Using  $\text{tr}[\sigma_j] = 0 \ \forall j$  and  $\sigma_z^2 = \mathbb{1}$ , (18) becomes  $1 = \frac{1}{2}(2\lambda + 2\alpha k_z) \ \forall \alpha \in [-1, 1]$ , which immediately yields  $k_z = 0$ ,  $\lambda = 1$  and  $k_x^2 + k_y^2 \leq 1$ . Thus,

$$M_0 = \mathbb{1} + r(\cos \theta \sigma_x + \sin \theta \sigma_y) \quad (19)$$

for some setup-dependent  $r \in [0, 1]$  and  $\theta \in [0, 2\pi)$ . The initial rotation labeled with the angle 0 can be chosen arbitrarily, so we can set  $\theta = 0$  which yields the assertion.

### B. Determining the detector contrast $r$ experimentally

As we have seen in III, an RoC measurement device can be described by the POVM  $\{U_\varphi M_0 U_\varphi^* \mid \varphi \in [0, 2\pi), M_0 = \mathbb{1} + r\sigma_x\}$ . We can determine the detector contrast  $r$  as follows: Assume we have a source emitting a reliably linearly polarized state  $\rho_a = \frac{a}{2}\mathbb{1} + (1-a)|H\rangle\langle H|$  for some known  $a \in [0, 2]$ , where  $|H\rangle$  denotes a horizontally polarized state. By measuring in the linearly polarized basis, we can determine the quotient of the number of horizontally and vertically polarized measurement outcomes

$$\frac{N_H}{N_V} = \frac{\text{tr}[\rho M_0]}{\text{tr}[\rho M_{\pi/2}]} \quad (20)$$

Since we have not yet used our freedom of orienting the Bloch sphere, we will do so now. The polarization’s rotation along the propagation direction is a subgroup of  $\text{SO}(3)$ , which has a  $\text{SU}(2)$  representation. We choose the xy-rotation of the polarization to correspond to the  $\pm \sigma_x$ -direction in the Bloch sphere, i.e.

$$|V\rangle\langle V| = \frac{\mathbb{1} + \sigma_x}{2} \quad \text{and} \quad |H\rangle\langle H| = \frac{\mathbb{1} - \sigma_x}{2}. \quad (21)$$

Then, one can explicitly derive the term (20), namely

$$\begin{aligned} \text{tr}[\rho_a M_0] &= \text{tr}[\rho_a (\mathbb{1} + r\sigma_x)] = 1 + r(a - 1) \\ \text{tr}[\rho_a M_{\pi/2}] &= \text{tr}[\rho_a e^{i\frac{\pi}{2}\sigma_z} (\mathbb{1} + r\sigma_x) e^{-i\frac{\pi}{2}\sigma_z}] \\ &= 1 - r(a - 1), \end{aligned} \quad (22)$$

which yields

$$r = \frac{N_H/N_V - 1}{(N_H/N_V + 1)(a - 1)}. \quad (23)$$

### C. Deriving the SDP Formulation

We show that (6) can be formulated as the SDP in (7): Any hermitian operator  $A$  can be divided into two positive semidefinite operators  $A_+$  and  $A_-$  such that  $A = A_+ - A_-$ . Since the trace norm equals the sum of the eigenvalues’ absolute values, we obtain

$$\|\rho^\Gamma\|_1 = \text{tr}[\rho_+^\Gamma] + \text{tr}[\rho_-^\Gamma] = 2 \text{tr}[\rho_+^\Gamma] - \text{tr}[\rho_-^\Gamma] = 2 \text{tr}[\rho_+^\Gamma] - 1.$$

Hence,  $\mathcal{N}(\rho) = \text{tr}[\rho_+^\Gamma] - 1$ . By applying Lemma 1, we immediately obtain the form in (7).

#### D. Error Estimation for RoC Measurements

Assume that we perform  $n$  measurements in an RoC setting yielding I.I.D. random variables  $X_1, X_2, \dots, X_n$ . This means assuming that our measurement device does not change over time and that the different shots do not influence each other. Under this assumption, we can apply Hoeffding's inequality [37], namely

$$\mathbb{P}\left(\left|\sum_{i=1}^n X_i - \mu\right| \geq \varepsilon\right) \leq 2 \exp\left\{-\frac{2\varepsilon^2}{\sum_{i=1}^n (b_i - a_i)^2}\right\} \forall \varepsilon > 0, \quad (24)$$

where  $\mu$  is the expectation value of the underlying probability distribution, and  $a_i \leq X_i \leq b_i$  almost surely (i.e. the probability that  $X_i$  lies in this range is 1).

Having simultaneously performed RoC measurements at angle segment  $\Delta\varphi_i$  on Alice's qubit and at  $\Delta\varphi_j$  on Bob's qubit, the probability for a detection event is given by  $P_{ij} = \text{tr}[\rho(A_i \otimes B_j)]$ . Measuring  $n$  times, we obtain a list  $(X_1, \dots, X_n)$ , where  $X_k = 1$  if the  $k$ 'th measurement detected an event in the chosen angle segments of Alice and Bob and  $X_k = 0$  otherwise. Hence, the measured frequency is  $p_{ij} = \sum_{k=1}^n X_k/n$  and in the above notation, we have  $a_k = 0$  and  $b_k = 1$  for all  $k$ . Therefore, (24) becomes

$$\mathbb{P}(|p_{ij} - P_{ij}| \geq \varepsilon) \leq 2e^{-\frac{2}{n}\varepsilon^2} \quad \forall \varepsilon > 0. \quad (25)$$

Now we can choose a confidence level  $c \in [0, 1]$ , 1 meaning we have a 100% confidence that the bound holds. Then, by (25), we know with certainty  $c$  that our measured frequency deviates by less than  $\sqrt{\frac{n}{2} \ln \frac{2}{1-c}}$  from the theoretical probability, i.e.,

$$\mathbb{P}\left(|p_{ij} - P_{ij}| < \sqrt{\frac{n}{2} \ln \frac{2}{1-c}}\right) > c. \quad (26)$$

#### E. Example for Semi-device Independent Entanglement detection

Fig. 2 shows one example of entanglement detection, where we assume that we have identical sample devices  $r_A = r_B$ . The full detection scheme, as explained in VI, considers all hypothetical devices and not only the optimal one. Fig. 6 explains, how this is done in more detail.

#### F. Deriving Minimal $(r_A, r_B)$ for Detecting Entanglement

The maximally entangled state  $|\Psi^-\rangle\langle\Psi^-|$  is the Werner state  $W_f = f|\Psi^-\rangle\langle\Psi^-| + \frac{1-f}{4}\mathbb{1}$  with  $f = 1$ . The probability of a detection event in angles  $\varphi$  and  $\psi$  is

$$\text{tr}[W_f(M_\varphi^{r_A} \otimes M_\psi^{r_B})] = \frac{1 - f r_A r_B \cos[2(\varphi - \psi)]}{\pi^2}, \quad (27)$$

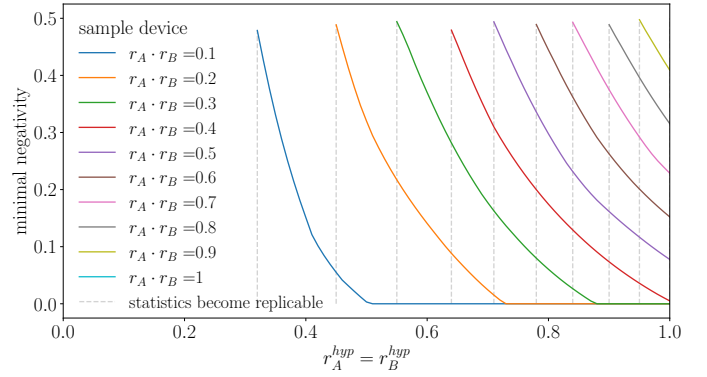


FIG. 6. Entanglement detection for unknown sample devices, assuming that  $r_A = r_B$ . The minimal negativities result from solving SDP (7) (using 'MOSEK'-solver in CVXPY). Statistics  $\{p_{ij}\}$  are simulated with the maximally entangled sample state  $|\Psi^-\rangle\langle\Psi^-|$  and several sample devices. Each colored line represents the minimized negativities for all hypothetical devices. The left-hand side of the dotted lines represents case 1. Those for which the minimized negativity is positive represent case 2. Those for which it reaches zero represent case 3. Entanglement is detected for sample devices with  $r_A r_B \geq 0.4$ .

where we use the POVM elements as defined in (2). This shows that having a Werner state with fidelity  $f$  and a measurement device defined by  $(r_A, r_B)$  is equivalent to having an ideal measurement device (i.e.  $r_A = r_B = 1$ ) and a Werner state with fidelity  $\tilde{f} = f r_A r_B$ . Given the probability  $P_{\varphi, \psi}$  for  $\psi = \varphi = 0$  from an experiment, using (27), we can easily determine  $\tilde{f} = 1 - 4\pi^2 P_{00}$ . A Werner state is entangled, iff its fidelity  $\tilde{f} > 1/3$ . Hence, given a maximally entangled state ( $f = 1$ ) and the statistics, in order to detect entanglement, the detector contrasts  $(r_A, r_B)$  must be at least

$$r_A r_B > \frac{1}{3}. \quad (28)$$

#### G. Pauli-Measurements with RoC-Devices

Let Bob's RoC device be defined by detector contrast  $r$ . We can define two measurement devices, as in (5) by partitioning the angles horizontally (i.e.  $\{\Delta\varphi_i^y\} = \{[0, \pi/2], [\pi/2, \pi]\}$ ) and vertically (i.e.  $\{\Delta\varphi_i^x\} = \{[\pi/4, 3\pi/4], [0, \pi/4] \cup [3\pi/4, \pi]\}$ ). Define the operators

$$A^y = \frac{1}{\pi} \int_0^{\pi/2} M_\varphi^r d\varphi, \quad B^y = \frac{1}{\pi} \int_{\pi/2}^{\pi} M_\varphi^r d\varphi \quad (29)$$

and  $A^x, B^x$  respectively. A simple calculation shows that  $\frac{\pi}{2r}(B^x - A^x) = \sigma_x$  and  $\frac{\pi}{2r}(B^y - A^y) = \sigma_y$ . Thus, if the value of  $r$  is known, post-processing enables measurements of  $\sigma_x$ .

## H. Parent POVMs imply LHV Models

We say that a POVM  $\{M_\lambda\}_\lambda$  is a *parent POVM* of a family of POVMs  $\{\{A_x^i\}_{x \in S_i} | i \in I\}$  if, for all  $i$  and  $x$ , we can write  $A_x^i = \int d\lambda a_\lambda^{x|i} M_\lambda$ , for some  $a_\lambda^{x|i} \geq 0$ .

According to the Naimark Theorem [39, 51] any POVM  $\{M_\lambda\}_\lambda$  on a Hilbert space  $\mathcal{H}$  can be extended to a projection valued measure (PVM)  $\{P_\lambda\}_\lambda$  on a Hilbert space  $\mathcal{K}$  of higher dimension and there exists a projection  $V : \mathcal{H} \mapsto \mathcal{K}$  such that  $M_\lambda = V^* P_\lambda V$ . Note:  $V$  is an isometry on the subspace  $\mathcal{H} \subset \mathcal{K}$ , i.e.  $V^* V = \mathbb{1}$ .

Let  $\{M_\lambda^A\}_\lambda$  be the parent POVM for Alice's POVMs  $\{A_x^i\}_x$  and  $\{M_{\tilde{\lambda}}^B\}_{\tilde{\lambda}}$  for Bob's  $\{B_y^j\}_y$ . Applying the Naimark theorem for both, we obtain the isometry  $V = V^A \otimes V^B$  such that  $P_\lambda^A \otimes P_{\tilde{\lambda}}^B = V(M_\lambda^A \otimes M_{\tilde{\lambda}}^B)V^*$  are projections. The probability of Alice measuring  $x$  in measurement  $i$  and Bob measuring  $y$  in measurement  $j$  is:

$$\begin{aligned} \mathbb{P}(x, y | i, j) &= \text{tr}[\rho(A_x^i \otimes B_y^j)] \\ &= \int d\lambda \int d\tilde{\lambda} a_\lambda^{x|i} b_{\tilde{\lambda}}^{y|j} \text{tr}[\tilde{\rho}(P_\lambda \otimes P_{\tilde{\lambda}})] \\ &= \int d\gamma a_\gamma^{x|i} b_\gamma^{y|j} \mathbb{P}(\gamma) \end{aligned} \quad (30)$$

where  $\tilde{\rho} = V\rho V^*$  and  $\gamma = (\lambda, \tilde{\lambda})$ . Considering

$$\mathbb{1} = \sum_x A_x^i = V^* \left( \int d\lambda \left( \sum_x a_\lambda^{x|i} \right) P_\lambda^A \right) V \quad (31)$$

and the fact that  $V$  acts as the identity on the subspace  $\mathcal{H}$ , from the orthogonality of the  $P_\lambda^A$  follows that  $\sum_x a_\lambda^{x|i} = 1$  and, analogously,  $\sum_y b_\lambda^{y|i} = 1$ . Hence,  $a_\lambda^{x|i}$  are probabilities for obtaining outcome  $x$ , when given measurement  $i$  and  $\lambda$ , which shows that we have found an LHV model in (30).

In our case  $\{M_\varphi^{r_A}\}_{\varphi \in [0, \pi)}$  and  $\{M_\varphi^{r_B}\}_{\varphi \in [0, \pi)}$  as in (2) are the parent POVMs for the Bell measurements

$$\begin{aligned} \{A_x^i\}_x &= \left\{ \int_{\varphi \in \varphi_x^i} M_\varphi^{r_A} \mid x \in X_i \right\} \\ \{B_y^j\}_y &= \left\{ \int_{\varphi \in \Psi_y^j} M_\varphi^{r_B} \mid y \in Y_j \right\}, \end{aligned} \quad (32)$$

where  $X_i$  and  $Y_j$  are index sets and  $\cup_{x \in X_i} \varphi_x^i = \cup_{y \in Y_j} \Psi_y^j = [0, \pi)$ . Note that the typical CHSH setting is obtained for  $i, j \in \{1, 2\}$  and  $X_i = Y_j = \{0, 1\}$  by assigning  $+1$  to the first measurement outcome and  $-1$  to the second outcome, for both POVMs, respectively.

## I. Comparison to Klein–Nishina

Fixing the azimuthal angle  $\theta$  and the energy quotient  $\beta$  in the Klein–Nishina formula for linearly polarized light

(11), the probability of finding a photon in angle  $\varphi$  is

$$\begin{aligned} \mathbb{P}_{\beta, \theta}(\varphi) &= \frac{I(\varphi)}{\int_0^\pi I(\gamma) d\gamma} \\ &= \frac{2 \sin^2 \varphi (1 + \beta (1 - \cos \theta)) + \beta^2 (1 - \cos \theta)^2}{\pi [1 + \beta (1 - \cos \theta) + \beta^2 (1 - 2 \cos \theta + \cos \theta)^2]}. \end{aligned} \quad (33)$$

For a maximally linearly polarized state  $\rho = \frac{1}{2}(\mathbb{1} - \sigma_x)$ , our RoC description yields the probability

$$\mathbb{P}_r^{RoC}(\varphi) = \frac{1}{\pi} \text{tr}[\rho U_{-\varphi} M_0 U_\varphi] = \frac{1 - r \cos(2\varphi)}{\pi}. \quad (34)$$

Solving the equation  $\mathbb{P}_r^{RoC}(\varphi) = \mathbb{P}_{\beta, \theta}(\varphi) \quad \forall \varphi \in [0, \pi)$  for  $r$  yields equation (12).

## Appendix A: Appendix

**Lemma 1.** *Let  $A$  be a hermitian operator on a finite dimensional Hilbert space  $\mathcal{H}$ . Then*

$$\text{tr}[A_+] = \inf_{T \in \mathcal{T}} \text{tr}[T] \text{ with } \mathcal{T} = \{T : \mathcal{H} \rightarrow \mathcal{H} \mid T \geq 0, T \geq A\}.$$

*Proof.* If  $A = A_+$  we know that  $A$  is positive and the statement is trivial. Assume that  $A_+ > A$ . We have  $A_+ \in \mathcal{T}$ , because  $A_+ \geq A$  and  $A_+ \geq 0$ . Hence, it is left to show that there cannot exist a  $T \in \mathcal{T}$  s.t.  $\text{tr}[T] < \text{tr}[A_+]$ . Assume there was such a  $T$ .

Let  $\vec{a}_1, \dots, \vec{a}_n$  be an orthonormal basis of eigenvectors of  $A$  with real eigenvalues  $\alpha_1, \dots, \alpha_n$  and let it be ordered such that  $\alpha_i > 0$  for  $i \leq n_+$  and  $\alpha_i \leq 0$  for  $i > n_+$ . Since  $T \geq A$ , for all  $i \leq n_+$  we have

$$0 \leq \vec{a}_i^* (T - A) \vec{a}_i = \vec{a}_i^* (T - A_+) \vec{a}_i = \vec{a}_i^* T \vec{a}_i - \alpha_i \quad (\text{A1})$$

Now since  $A_+$  is the part of  $A$  carrying the positive eigenvalues, we have  $A_+ \vec{a}_i = 0$  for all  $i \geq n_+$ . Therefore,

$$\begin{aligned} 0 > \text{tr}[T - A_+] &= \sum_{i=1}^{n_+} \vec{a}_i^* (T - A_+) \vec{a}_i + \sum_{i=n_++1}^n \vec{a}_i^* (T - A) \vec{a}_i \\ &= \sum_{i=1}^{n_+} \vec{a}_i^* T \vec{a}_i - \alpha_i + \sum_{i=n_++1}^n \vec{a}_i^* T \vec{a}_i \geq 0 + 0, \end{aligned} \quad (\text{A2})$$

where the last inequality comes from (A1) and the fact that  $T \geq 0$ . This contradiction yields the assertion.  $\square$

Entanglement hides  
in circular symmetries  
lemonade finds.